Available online at www.sciencedirect.com
SCIENCE DIRECT®
Journal of Solid State Chemistry 178 (2005) 85–92
JOURNAL OF SOLID STATE CHEMISTRY
www.elsevier.com/locate/jssc

CTAB-assisted fabrication of mesoporous composite consisting of wormlike aluminosilicate shell and ordered MSU-S core

Shang-Ru Zhai[a], Jun-Lin Zheng[a], Dong Wu[a], Yu-Han Sun[a,*], Feng Deng[b]

[a]*State Key Laboratory of Coal Conversion, Institute of Coal Chemistry, Chinese Academy of Sciences, Number 27, Taoyuan Nan Lu, Taiyuan City, Shanxi Province 030001, PR China*

[b]*State Key Laboratory of Magnetic Resonance and Atomic Molecular Physics, Institute of Physics and Mathematics, Chinese Academy of Sciences, Wuhan 430071, PR China*

Received 26 March 2004; received in revised form 19 September 2004; accepted 26 September 2004

Abstract

Novel mesoporous composites comprised of aluminosilicate shell with wormhole framework structure and well-ordered MSU-S core have been firstly prepared via treatment of MSU-S with $NaAlO_2$ solution in the presence of cationic surfactant cetyltrimethylammonium bromide (CTAB). The obtained products were thoroughly characterized by XRD, HRTEM, N_2 sorption isotherm, TG-DSC, ^{27}Al MAS NMR and ^{29}Si MAS NMR, etc. Characterization results based on these techniques revealed that the introduction of CTAB during the treatment process played a crucial role in the formation of mesoporous composite, otherwise the parent ordered MSU-S would be completely destroyed. Furthermore, aluminum content in the final product determined by ICP and EDAX was significantly increased compared to the parent MSU-S, thus assuming that CTAB added in this modification process led a key role in the introduction of Al into the final solid via self-assembly with additionally added AlO_2^- and partly dissolved silicate species from the parent MSU-S particles. In addition, acidity and catalytic performance of the prepared mesoporous composite were also substantially improved in comparison to the parent MSU-S sample.

Keywords: Mesoporous; Core/shell structure; Composite; Catalysis

1. Introduction

Since the first reported syntheses of M41S family, there has been intense research activity in designing and synthesizing various micro/mesoporous and meso/mesoporous composites in that a hierarchical combination of independently controlled, well-connected smaller and larger pores reduces transport limitations in catalysis, resulting in higher activities and better controlled selectivities, and some fascinating discoveries have been reported in the previous studies [1–10]. For instance, Kloetstra [1] reported a bi-porous composite with a thin layer of MCM-41 overgrowth on FAU crystals by successive synthesis of FAU and MCM-41, wherein the sodium content appeared to induce the zeolite crystallization. In addition, Bein et al. [2] prepared nanosized micro/mesoporous composites via simultaneous synthesis of Beta/MCM-48 phases using two-template approach under optimized silica source, Si/Al ratio, template concentration and reaction temperature conditions. Moreover, a Beta/MCM-41 composite with bimodal pore structure and dual acidity obtained by two-step crystallization has also been presented [3]. Authentically, there are still many studies reported on the synthesis of micro/mesoporous composites [4–8]. However, although impressive progress has been made on the fabrication of micro/mesoporous composites [1–8], few literatures reported on the synthesis of structured mesoporous composites with potential applications in catalysis and separation [9,10], say nothing of

*Corresponding author. Fax: +86 351 404 1153.
E-mail address: yhsun@sxicc.ac.cn (Y.-H. Sun).

0022-4596/$ - see front matter © 2004 Elsevier Inc. All rights reserved.
doi:10.1016/j.jssc.2004.09.034

core/shell-structured mesoporous composite with high acidity and catalytic properties.

In this work, novel mesoporous composites comprising with hexagonally ordered MSU-S core and wormhole-like aluminosilicate shell were prepared via treatment of the parent MSU-S with $NaAlO_2$ solution in the appearance of cationic surfactant CTAB under hydrothermal conditions. The unique structure of the obtained product was clearly confirmed by XRD, HRTEM, N_2 adsorption isotherm, ^{27}Al MAS NMR and ^{29}Si MAS NMR. Furthermore, it was interesting that the acidity and catalytic activity of the composite structure were substantially improved in comparison to the parent MSU-S sample. At the same time, the effect of CTAB addition during the modification process on the core/shell structure formation was also discussed in detail.

2. Experimental section

2.1. Synthesis of the parent MSU-S

The parent MSU-S material was prepared hydrothermally, mainly following the method described by Pinnavaia et al. [11]. In a typical synthesis, after 0.507 g of NaOH and 0.352 g of $NaAlO_2$ were dissolved into 10 mL distilled water, 25.578 g of sodium silicates powder was added slowly under vigorous stirring at 35 °C until homogenize. After continuous stirring at this temperature for at least 4 h, the obtained clear solution was transferred into an autoclave and statically heated at 110 °C for 12 h. The parent MSU-S mesostructure (Si/Al = 20) was assembled by adding, under moderate stirring, appropriate amounts of preformed aluminosilicate units to the solution of CTAB template in distilled water at room temperature. The pH of the system was then adjusted to pH 9–10 by dropwise introducing determined amount of dilute H_2SO_4 solution (6 M) under vigorous stirring. Then the resultant gel was crystallized in a sealed autoclave at 140 °C for 48 h under static conditions. After the precipitates being filtered, washed thoroughly with distilled water, dried and calcined in air at 550 °C for 6 h, the parent MSU-S was obtained and designed as sample PM (parent material).

2.2. Preparation of mesoporous composite

In brief, 0.6074 g of CTAB and predetermined 0.2459 and 0.3687 g, respectively, of $NaAlO_2$ (concentration, 0.10 and 0.15 M, respectively) were dissolved into 30 mL distilled water to gain a clear solution at room temperature. Then 0.5 g of parent MSU-S was quickly added. After further stirring for 4–6 h at room temperature, the gel was transferred into a 40 mL Teflon-lined stainless steel autoclave and heated at 110 °C for 12 h. After cooling to room temperature, the solids were collected by filtration, washed with distilled water and dried in air at 80 °C. Treatment of the parent MSU-S (PM) and composite samples with 1.0 M NH_4NO_3 at 80 °C for 12 h to displace exchangeable sodium ions, then samples in the acid form were obtained by activation at 550 °C for 6 h. Corresponding to 0.10 M and 0.15 M $NaAlO_2$ used, the obtained composite structures were referred to as CM1 (composite material) and CM2, respectively.

To elucidate the important role of CTAB played in the formation of mesoporous composite, the well-ordered MSU-S was also treated by 0.10 M $NaAlO_2$ solution without CTAB, and this product was designated as NM (nonporous material).

2.3. Materials characterization

Powder X-ray diffraction patterns were measured using Ni filtered Cu Kα radiation ($\lambda = 1.5404$ Å) and a Rigaku D Max III VC diffractometer equipped with a rotating anode operated at 40 kV and 30 mA. Counts were accumulated every 0.02° (2θ) at a scan speed of 1° (2θ) per min.

TEM images were recorded using a JEOL 100CX microscope with a CeB6 filament and an accelerating voltage of 200 kV. Samples were prepared by sonicating the powdered sample for 15 min in ethanol and then evaporating two drops onto carbon-coated copper grids.

N_2 adsorption–desorption isotherms were obtained on a Tristar 3000 Sorptometer using static adsorption procedures at −196 °C. Samples were degassed at 150 °C and 10^{-6} Torr for minimum 12 h prior to analysis. BET surface areas were calculated from the linear part of the BET plot according to IUPAC recommendations. Pore size distributions were calculated from the N_2 adsorption branches using the conventional BJH model.

Aluminium content and element compositions in the materials were determined using ICP and EDAX capability of the SEM instrument on a Philips SEM 505 microscope.

^{27}Al MAS NMR spectra were performed on a Bruker MSL 500S spectrometer and recorded at 130.245 MHz with 1 μs pulse width, 1 s recycle delay time, and 10 kHz spinning speed. Spectra were recorded with an external reference of a totally octahedral 1.0 M $Al(NO_3)_3$ solution assigned 0 ppm chemical shift.

^{29}Si MAS NMR spectra were obtained using a DOTY Scientific multinuclear probe and 5 mm zirconia rotors: ^{29}Si resonance frequency, 99.745 MHz; pulse width, 4 μs; recycle delay time, 400 s; spinning speed, 8 kHz; reference to tetramethylsilane (TMS) assigned 0 chemical shift.

TG-DSC measurements were performed on a STA 409PC instrument under the condition of $O_2/N_2/50/10$ at a heating rate of 10 °C/min between 30 and 800 °C.

NH_3-TPD was performed in a quartz micro-reactor. A sample of 0.20 g was freshly heated in argon at 600 °C for 0.5 h. NH_3 was introduced to the sample after it was cooled down to 120 °C. To remove the weakly adsorbed NH_3, the sample was swept using argon at 120 °C for 2 h. The TPD experiments were then carried out with a carrier-gas flowing rate of 40 mL/min argon from 120 to 600 °C using a linear heating rate of 10 °C/min. The desorption of NH_3 was detected by Shimadzu GC-9A equipped with a TCD detector.

2.4. Cumene cracking reaction

Cumene cracking reactions were carried out at 300 °C by pulse method to evaluate catalytic performance of the composite and the parent MSU-S samples. In each run, 0.2 μL reactant was pulsed and cracked over 0.06 g of each catalyst, and nitrogen was used as carrier gas with a flowing rate of 50 mL/min. The reaction products were analyzed using GC-9A (Shimazu Co.) equipped with a FID detector and a high resolution Chrom-Workstation Data Set. GC was used to determine the reactant conversion.

3. Results and discussion

3.1. XRD analysis

Powder X-ray diffraction patterns of the PM, CM1, CM2 and NM samples are shown in Fig. 1. As observed in Fig. 1(a), the parent MSU-S material (PM) exhibits a strong (100) basal line and at least three higher order peaks, which are well associated with the ordered hexagonal symmetry of MCM-41-like mesostructures [11–13]. In contrast, for the present mesoporous composite CM1 shown in Fig. 1(b), the intensity of (100) diffraction peak decreases largely and the (100) and (200) peaks disappear completely, indicating that the pore structure of the present case is less uniform, lacking the long-range crystalline order in comparison to that of the initial MSU-S. More interestingly, the CM2 sample displays two well-resolved peaks at the lower angle, further and strongly suggesting a mesoporous composite material was obtained [10].

On the other hand, the sample (NM) obtained via treatment of the structurally ordered MSU-S with 0.10 M $NaAlO_2$ solution without CTAB under the present mesoporous composite formation conditions entirely loses its original mesoporous character, none of low-angle peaks is presented.

3.2. TEM observation

Corresponding to the above XRD observations, Fig. 2 displays the representative TEM images of the

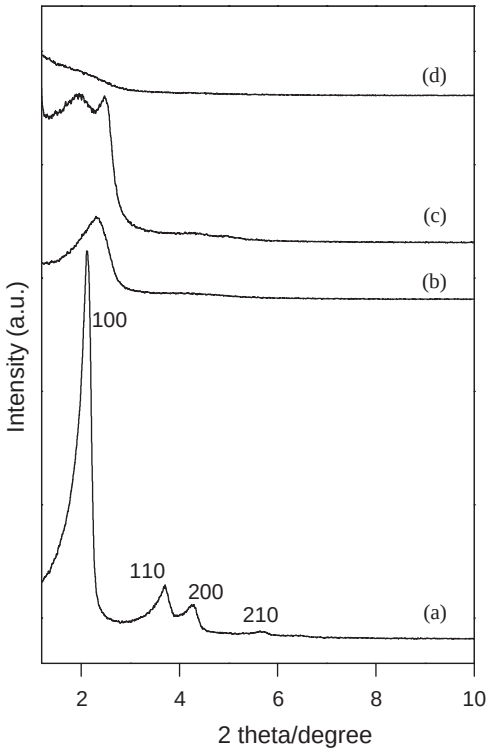

Fig. 1. XRD patterns of (a) sample PM; (b) sample CM1; (c) sample CM2; and (d) sample NM.

PM and CM1 samples. As illustrated in Fig. 1(a), TEM image for the parent MSU-S viewed down a direction perpendicular to the pore axis, showing regular parallel ordering of the pores and their continuity through the entire length of the particle. In contrast, it is clearly indicated that, from the TEM micrograph of the cross-sectional particles of the CM1 sample shown in Fig. 1(b), the present material is of well core/shell structure with a thin shell of estimated a few nanometers thick. Enlarged image for the region (c) in Fig. 1(b) further reveals that not only the ordered channels in the cores were retained during the modification process, but also an even aluminosilicate shell embedded with uniform mesopores in thickness about 15–20 nm was formed on the surface of cores. However, the pore structure of the cores is not nearly ordered as the starting PM sample may result from the intrusion of extremely little part of aluminosilicate deposited unevenly onto the inner pore walls of the parent MSU-S [14]. More interestingly, TEM photo of the shell microsectioned from the present composite CM1, as illustrated in Fig. 1(d), obviously demonstrates that the shells have a disordered wormhole-like pore structure, which is much less ordered than that of the interior of the particles. And, these accessible pores are connected randomly, lacking discernible long-range pore ordering in the shells, thus possibly leading to a very broad low-angle peak for CM1 sample via shown in Fig. 1(b).

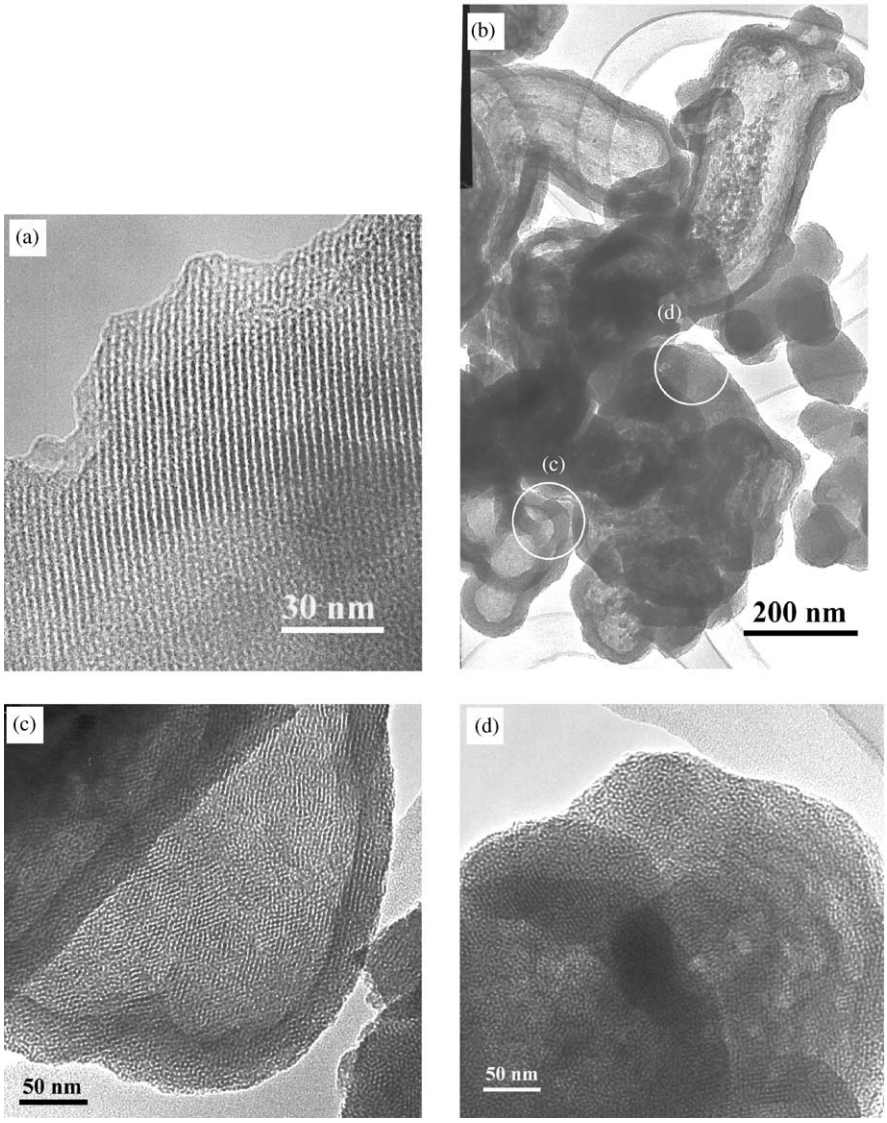

Fig. 2. TEM images of (a) sample PM and (b) sample CM1 at low magnification; (c) and (d) magnified images from the regions in (b).

3.3. N_2 adsorption measurement

Textural characteristics were evaluated from nitrogen adsorption–desorption isotherms at −196 °C. Fig. 3 displays the N_2 adsorption–desorption isotherms and corresponding pore size distributions of the PM, CM1 and NM materials. It is clearly observed that, from Figs. 3(a) and (b), the isotherms of both PM and CM1 samples are of classical type IV, characteristic of mesoporous materials according to the IUPAC classification [15]. Obviously, the adsorption isotherm of the PM sample exhibits a steep inflection point at $P/P_0 = 0.30-0.45$, typical of capillary condensation process within uniform mesopores [15–17]. This uniformity is also shown by the narrow pore size distribution

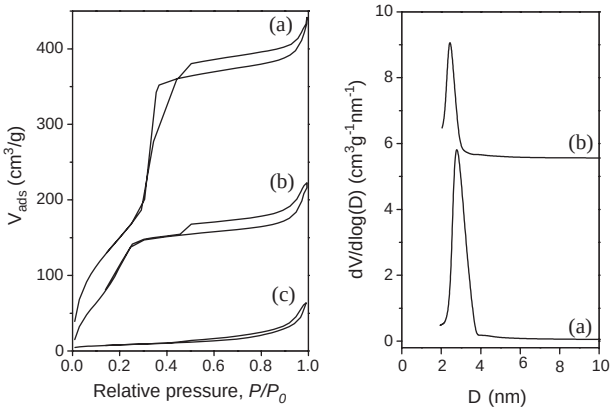

Fig. 3. Nitrogen adsorption–desorption isotherms and pore size distributions of (a) sample PM; (b) sample CM1; and (c) sample NM.

Table 1
Structural properties of the studied samples

Sample	a[a] (nm)	S_{BET} (m^2/g)	Pore size (nm)	V_p (cm^3/g)	Wall thickness[b] (nm)
PM	5.01	906	2.79	0.791	2.22
CM1	4.67	722	2.48	0.531	2.19
NM	—[c]	29	—	0.069	—

[a]Unit cell parameter from XRD data using the formula, $a = d_{100} \times (2/3^{1/2})$.
[b]Pore wall thickness, a—pore size.
[c]"—" means the data undetectable.

Table 2
Compositions of the typical composite and the parent MSU-S

Sample	Al content[a] (wt%)	O element[b] (at%)	Al element[b] (at%)	Si element[b] (at%)
PM	1.44	64.74	1.98	33.27
CM1	8.74	61.82	8.44	29.74

[a]Determined by ICP.
[b]Analyzed by EDAX.

calculated by the BJH method for cylindrical pores. However, for the present case of CM1 the inflection point position moves to lower P/P_0 range of 0.15–0.25 and the pore size reduces to 2.48 nm. Despite this, the pore size distributions of both samples depicted in Fig. 3 are quite uniform, revealing the good homogeneity of the mesopores.

As listed in Table 1, although the BET surface area and total pore volume of the CM1 in comparison to the PM sample slightly decreases from 906 to 722 m^2/g and 0.791 to 0.531 cm^3/g, respectively, the pore wall thickness of the CM1 is almost identical to that of the PM sample. This is indicated that the unit cell reduction can be almost entirely attributed to a decrease in pore size. However, it should be noted that the present CM1 possesses the classic advantages of high surface area, porosity and uniform pore size as the typical MCM-41 mesoporous silicas [18,19], though there is slight decrease of specific surface area and pore volume relative to the PM. Although the detailed explanation for these results is not clear at the present time, we speculate that the strong interaction between the charge balancing surfactant molecules and the framework aluminum sites caused contraction of the mesoporous framework, resulting in the decrease of pore volume and specific surface area [14].

As shown in Fig. 3(c), it is noteworthy that the N_2 adsorption isotherm of the NM material exhibits virtually no mesostructured character, which is well consistent with its XRD result. Furthermore, the surface area and pore volume of it in comparison to the parent MSU-S is decreased by 96% and 91%, respectively. It is thus considered that CTAB added in the modification process authentically acted as a protector to the pore framework of the initial MSU-S, otherwise the original well-ordered MSU-S would be entirely destroyed.

3.4. Effect of CTAB in the composite formation

To further study the role of CTAB played in the composite formation, the compositions of the representative composite CM1 and the parent MSU-S was analyzed and compared (see Table 2). It is clearly seen from this Table that aluminum content in the CM1 sample is substantially higher than that of the parent MSU-S, indicating large amount of aluminum has been introduced into the final composite. And, the coordination of Al atoms in the CM1 and PM was probed and compared by ^{27}Al NMR spectroscopy (see Fig. 4). It is interesting to observe that the additionally introduced Al has been mainly incorporated into the framework and this coordination symmetry is generally maintained with increasing aluminum content. At the same time, we also find that the oxygen and silicon content in the CM1 sample slightly decreases relative to the PM material. It is thus postulated that CTAB may play a crucial role in the introduction of Al into the final composite via self-assembly with additionally introduced AlO_2^- and partly dissolved silicates from the parent MSU-S particles.

As known, the mesostructured PM material was assembled from preformed zeolite seeds using the established S^+I^- micellar templating system under basic conditions [11–13,17]. It is therefore speculated that, if part of its particles was degraded and this part silicates was in situ self-assembled with CTAB and re-precipitated onto the surface of the retained particles under the present hydrothermal conditions, the intended reduced crystallinity of the obtained mesoporous composite over

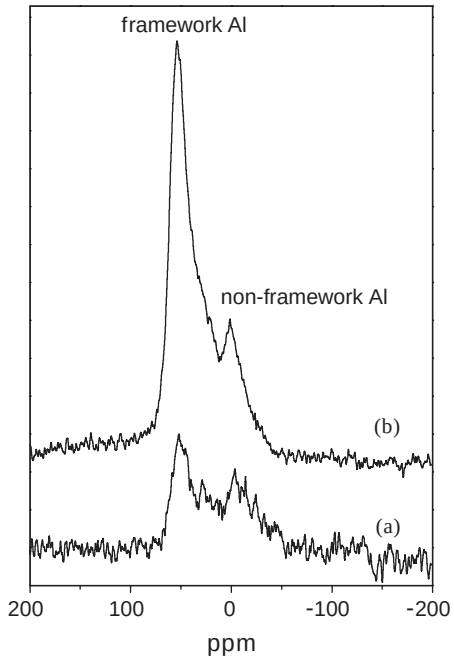

Fig. 4. ^{27}Al MAS NMR spectra of calcined (a) MSU-S (b) representative composite CM1.

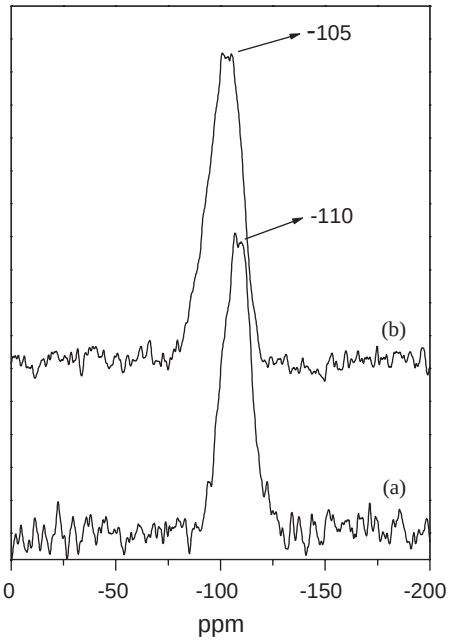

Fig. 5. ^{29}Si MAS NMR spectra of calcined (a) MSU-S (b) representative composite CM1.

the parent MSU-S be demonstrated in the ^{29}Si NMR spectra. It is reported that, in a typical silicate mesostructures, the amorphous nature of the frameworks implies there is continuum of SiO_x symmetries resulting in spectra that reflect various mixtures of Q^2, Q^3 and Q^4 Si coordination. The amorphous structures will possess high defect populations, therein causing the population of structural Q^3 silanol species to be significantly higher than the crystalline zeolite materials [12]. It will be noticed that the ^{29}Si NMR spectra of the CM1 and PM materials are somewhat different, that is, the spectral line and chemical shift of the CM1 are broader and higher than those observed in the parent MSU-S (see Fig. 5). This is a clear indication that the atomic structures of both aluminosilicate materials are slightly different. The inference can be drawn that, because of the spectral differences, the present structure is indeed composed of two different mesophases. In combination of the discussed XRD, TEM and N_2 sorption isotherm results, a novel core/shell structured composite is reliably obtained.

Differential thermal analysis of various mesostructures prepared with organic templates has been shown to provide information on the Si/Al ratios of the materials and the coordination environment of the template within the framework [3,12,20]. It seemed possible that the apparently different structure and aluminum content could modify the surface interactions between the surfactant molecules and silicate framework. Fig. 6 shows the TG-DSC curves of the as-synthesized CM1 and PM materials. As shown in Fig. 6A (a), the PM material exhibits a very sharp and high-intensity exotherm at approximately 300 °C, with a corresponding sharp weight loss. And this distinct observation should be mainly attributed to the thermo-desorption/decomposition of cationic CTAB, which is well consistent with the reported thermal results for the MSU-S [12]. Compared to the PM sample, the exotherm for the composite CM1 shifts to slightly higher temperature and appears to become much broader. This result can be reasonably assigned to the increased Al concentration and complicated coordination environment of CTAB molecules occluded in the framework of CM1 material [12]. The total weight losses due to CTAB removal from both PM and CM1 are roughly 32 and 38%, respectively, which is in agreement with their starting compositions.

Based on the above comprehensive characterizations, it is unambiguously concluded that the introduced CTAB authentically served as a template for the mesoporous aluminosilicate coating via self-assembly with additionally introduced AlO_2^- and partly degraded silicates from the parent MSU-S particles.

3.5. Acidity and catalytic properties

Ammonia TPD is widely used to determine the total acidity of solid acids. The amount of ammonia desorbed at some characteristic temperatures is taken as a measure of the number of acid centers while the temperature range in which the ammonia is desorbed is an indicator of the strength of the acid sites [21]. As

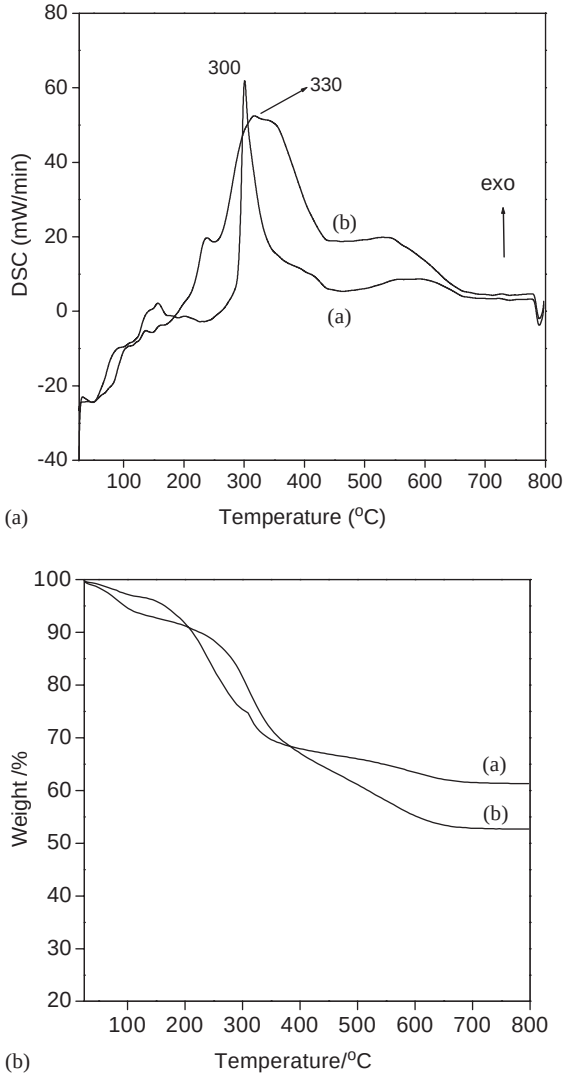

Fig. 6. TG-DSC profiles from room temperature to 800 °C of as-synthesized (a) MSU-S and (b) typical composite CM1.

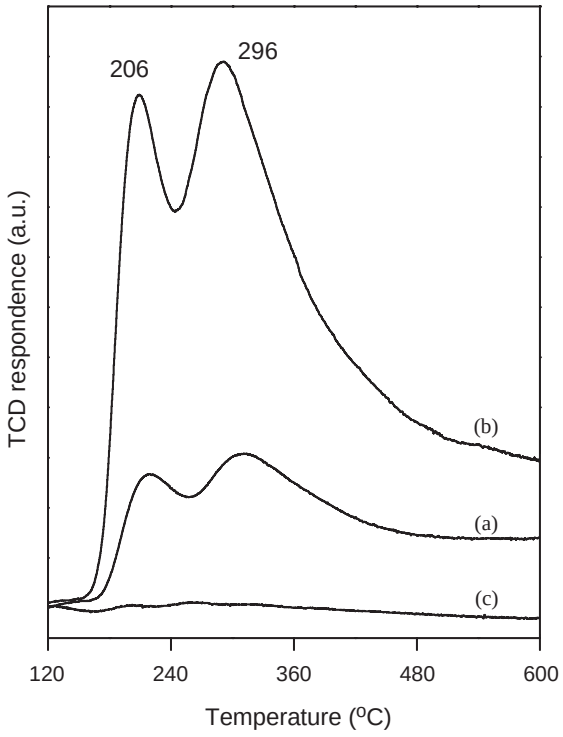

Fig. 7. NH_3-TPD curves of (a) sample PM; (b) sample CM1; and (c) sample NM in the acid forms.

Table 3
Activity in cumene cracking for the studied samples

Sample	Conversion[a] (mol%)	Selectivity			
		Propylene	Benzene	*m*-D[b]	*p*-D[c]
PM	6.184	30.44	69.55	—[d]	—
CM1	56.129	30.57	67.41	2.02	—
NM	—	—	—	—	—

[a]Conversions were the fifth run.
[b,c]Standing for *m*-diisopropylbenzene and *p*-diisopropylbenzene, respectively.
[d]The product was undetectable.

shown in Fig. 7(a), the amount of NH_3 adsorbed on the PM is very low. For sample CM1 however, substantially increased amount of adsorbed NH_3 is observed, obviously indicating more acid centers have been created. Furthermore, two NH_3 desorption peaks at ca. 206 and 296 °C are presented. This result indicates that the strength of the acid sites on the surface of PM and CM1 is mild [22]. In addition, no obvious peak-shift can be observed for the desorption of NH_3 though both samples having remarkably different Al content, showing the strength distribution of acid sites is quite similar. However, sample NM shows no acidity, which is well consistent with the fact that CTAB added in the present system played a key role in the formation of core/shell structure and therefore incorporation of Al species into the framework, otherwise the initial MSU-S would be completely destroyed and lost its acidity.

To further investigate the acidity of these materials, the catalytic cracking of cumene was chosen as test reaction [11–13], and catalytic results are given in Table 3. Noticeably, the composite CM1 exhibited excellent catalytic activities towards cumene conversion, and propylene and benzene were the main products. In addition, minor alkylation products such as *m*-diisopropylbenzene and *p*-diisopropylbenzene were also detected [12,23]. It is interesting to find that, combined with the textural parameters in Table 1, although the effective pore size, pore volume and specific surface area of the composite CM1 were slightly decreased in comparison to the parent MSU-S, there is a substantial improvement in cracking activity. It is thus considered that those additionally introduced Al species are easily

accessible to reactant, and this is a major advantage of the present composite material over those of directly synthesized mesostructured aluminosilicates. In the end, the NM product showed no catalytic activity, in agreement with its NH_3-TPD analysis.

4. Conclusions

In summary, novel mesoporous composites of worm-like aluminosilicate shell and ordered MSU-S core have been prepared via treatment of MSU-S with $NaAlO_2$ solution in the presence of CTAB. It is found that CTAB introduced in this system played an important role in the preparation of the core/shell structure, wherein it effectively cooperated with the modification agent $NaAlO_2$ and silicates partly degraded from the parent MSU-S particles and led to the overgrowth of a thin aluminosilicate layer on the retained MSU-S particles. This synthetic pathway provides an important example of fabrication of designed mesoporous composite with cell/shell structure, and these composite materials may find wide applications in catalysis and separation process.

Acknowledgments

Financial support from the National Key Basic Research Foundation (G 2000048001) and Natural Science Foundation (29973057) is gratefully acknowledged.

References

[1] K.R. Kloetstra, H.W. Zandbergen, J.C. Jansen, H. van Bekkum, Micropor. Mater. 6 (1996) 287.
[2] P. Prokesova, S. Mintova, J. Cejka, T. Bein, Micropor. Mesopor. Mater. 64 (2003) 165.
[3] W. Guo, L. Huang, P. Deng, Z. Xue, Q. Li, Micropor. Mesopor. Mater. 44–45 (2001) 427.
[4] K.R. Kloetstra, H. van Bekkum, C.T. Jacobus, Chem. Commun. 20 (1997) 2281.
[5] H. Liu, X. Bao, W. Wei, G. Shi, Micropor. Mesopor. Mater. 66 (2003) 117.
[6] A. Karlsson, M. Stocker, R. Schmidt, Micropor. Mesopor. Mater. 27 (1999) 181.
[7] D.T. On, D. Lutic, S. Kaliaguine, Micropor. Mesopor. Mater. 44–45 (2001) 435.
[8] L. Huang, W. Guo, P. Deng, Z. Xue, Q. Li, J. Phys. Chem. B 104 (2000) 2817.
[9] J. Sun, Z. Shan, T. Maschmeyer, J.A. Moulijn, M.O. Coppens, Chem. Commun. (2001) 2670.
[10] Y. Xia, R. Mokaya, J. Mater. Chem. 13 (2003) 3112.
[11] Y. Liu, W. Zhang, T.J. Pinnavaia, J. Am. Chem. Soc. 122 (2000) 8791.
[12] S.A. Bagshaw, S. Jaenicke, C.G. Khuan, Ind. Eng. Chem. Res. 42 (2003) 3989.
[13] Y. Liu, T.J. Pinnavaia, J. Mater. Chem. 12 (2002) 3179.
[14] R. Mokaya, Chem. Commun. (2000) 1541.
[15] K.S.W. Sing, D.H. Everett, R.A.W. Haul, L. Moscow, R.A. Pinerotti, J. Rouquerol, T. Siemieniewska, Pure Appl. Chem. 57 (1985) 603.
[16] Y. Zhang, X. Qian, Z. Li, J. Yin, Z. Zhu, J. Solid State Chem. 177 (2004) 844.
[17] S.A. Bagshaw, S. Jaenicke, C.G. Khuan, Catal. Commun. 4 (2003) 140.
[18] C.T. Kresge, M.E. Leonowicz, W.J. Roth, J.C. Vartuli, J.S. Beck, Nature 359 (1992) 710.
[19] J.S. Beck, J.C. Vartuli, W.J. Roth, M.E. Leonowicz, C.T. Kresge, K.D. Schmitt, C.T.W. Chu, D.H. Olsen, E.W. Sheppard, S.B. McCullen, J.B. Higgins, J.L. Schlenker, J. Am. Chem. Soc. 114 (1992) 10834.
[20] M. Kruk, A. Sayari, M. Jaroniec, Stud. Surf. Sci. Catal. 129 (2000) 567.
[21] E.R. Castellon, A.J. Lopez, P.M. Torres, D.J. Jones, J. Roziere, M. Trombetta, G. Busca, M. Lenarda, L. Storaro, J. Solid State Chem. 175 (2003) 159.
[22] Y.S. Ko, W.S. Ahn, Micropor. Mesopor. Mater. 30 (1999) 183.
[23] S.R. Zhai, W. Wei, D. Wu, Y.H. Sun, Catal. Lett. 89 (2003) 261.